Electronic Supporting Information

Lorentz Force-Assisted Growth of Romanesco-Like Ni-Fe Nano-Cone Arrays for Enhanced Oxygen Evolution Reaction at High Current Densities

Hongjie Liu,[a] Yunyi Jia,[a] Shunhang Hua,[a] Jingjing Weng,[a] Lumeng Wang,[a] Cheng Yang *[a]

[a] Institute of Materials Research, Tsinghua Shenzhen International Graduate School, Tsinghua University, Shenzhen 518055, PR China.

Experiment section

Preparation of Romanesco-like Ni-Fe nanocone arrays on Ni foam

The Romanesco-like Ni-Fe arrays were fabricated through a one-step electrodeposition process. A commercial nickel foam (thickness: 1.5 mm, bulk density: 0.19 g cm^{-3}) was used as the substrate. All solutions in the experiments were prepared using analytical grade chemicals and deionized water. Before electrodeposition, the nickel foam was first sonicated in 2.0 M HCl solution for 5 minutes to remove the NiO_x layer on the surface, followed by rinsing with water and ethanol, and then dried in air. The electrodeposition was carried out in a two-electrode electrochemical cell under an applied vertical magnetic field, with the current direction perpendicular to the magnetic field. The nickel foam served as the working electrode, along with a parallel platinum plate auxiliary electrode. To obtain Romanesco-like Ni-Fe nanocone arrays, an electrolyte solution containing 0.84 M $NiCl_2 \cdot 6H_2O$, 0.65 M H_3BO_3, 1.86 M NH_4Cl, and 0.39 M $FeCl_2$ was used, with the pH adjusted to 4.0 using 10 % HCl and 10 % NH_4OH solutions. The electrodeposition was conducted at 60 ºC with a DC power source, applying a current density of 20 mA cm^{-2} and a magnetic field strength of 300 Gs, for a duration of 15 minutes. After deposition, the samples were carefully withdrawn from the electrolyte, thoroughly rinsed with water and ethanol, and left to dry in air. The growth of NiFe NCAs on nickel foam followed the same process as described above, except with no applied magnetic field. The growth of Ni NCAs on nickel foam was conducted in the absence of the applied magnetic field and without $FeCl_2$ in the electrolyte solution, with a deposition time of 15 minutes.

Materials characterization

The morphology of catalysts was characterized by field emission scanning electron microscopy (FE-SEM, SAPPHIRE SUPRA 55) and TEM (Jeol ARM 200F, Japan). Crystallographic information was obtained with X-ray diffraction (Bruker DSRINT2000/PC, Germany) using Cu Kα radiation with λ=1.5418 Å (at a diffraction

angle ranging from 30° to 80° at a scan rate of 5°/min). The X-ray photoelectron spectra (XPS) were measured with AlKα radiation (50 W, 15 kV) (ESCALABSB 250 Xi). An argon ion beam etching process was employed at an accelerating voltage of 2.0 kV.

Electrochemical measurement

Electrochemical measurements were conducted with electrochemical working station (CHI 660E) in a three-electrode electrochemical setup. A 1 M KOH solution was used as electrolyte, and an Hg/HgO electrode (in 1 M KOH) and graphite rod (with a diameter of 8 mm) were used as reference and counter electrodes, respectively. The as-prepared electrodes supported on Ni foam were utilized as the working electrode. The working area was tailored to 0.4 cm^2 . The relation between the Hg/HgO reference and RHE in 1 M KOH solution follows the formula ERHE = $E_{Hg/HgO}$+0.059 pH+0.095 V. The iR compensation was performed by automatic current interrupt method with a value of 93% x Ru through the CH instrument 660E working station. For OER, in order to provide reliable electrochemical data and avoid overlap between Ni^{2+}/Ni^{3+} oxidation and OER, polarization curves were recorded from high initial potentials to low final potentials with a 5 mV s^{-1} scan rate. Tafel slopes were calculated using the 3 polarization curves by plotting overpotential against log (current density). Chronopotentiometry measurements were performed to evaluate the long-term stability. The ECSA was determined by measuring the capacitive current associated with double-layer charging from the scan-rate dependence of CVs. For this, the potential window of CVs was - 0.1-0 V versus Hg/HgO. The scan rates were 20, 40, 80, 160, 240, 320 and 400 mV s^{-1} . The double-layer capacitance (C_{dl}) was estimated by plotting the $\Delta J = (Ja\text{-}Jc)$ at -0.05V versus Hg/HgO against the scan rate. The linear slope is twice of the double layer capacity. The ECSA values were calculated from the measured double layer capacitance divided by the specific capacitance of an atomically smooth material (Cdl ′, ~40 μF cm^{-2}): ECSA = Cdl÷Cdl′×S, where S is the actual surface area of the electrode. The electrochemical impedance spectroscopies (EIS)

measurement was conducted at 1.53 V (vs. RHE), in the frequency range of 100 kHz to 0.1 Hz with an amplitude of 5 mV.

Additional Figure

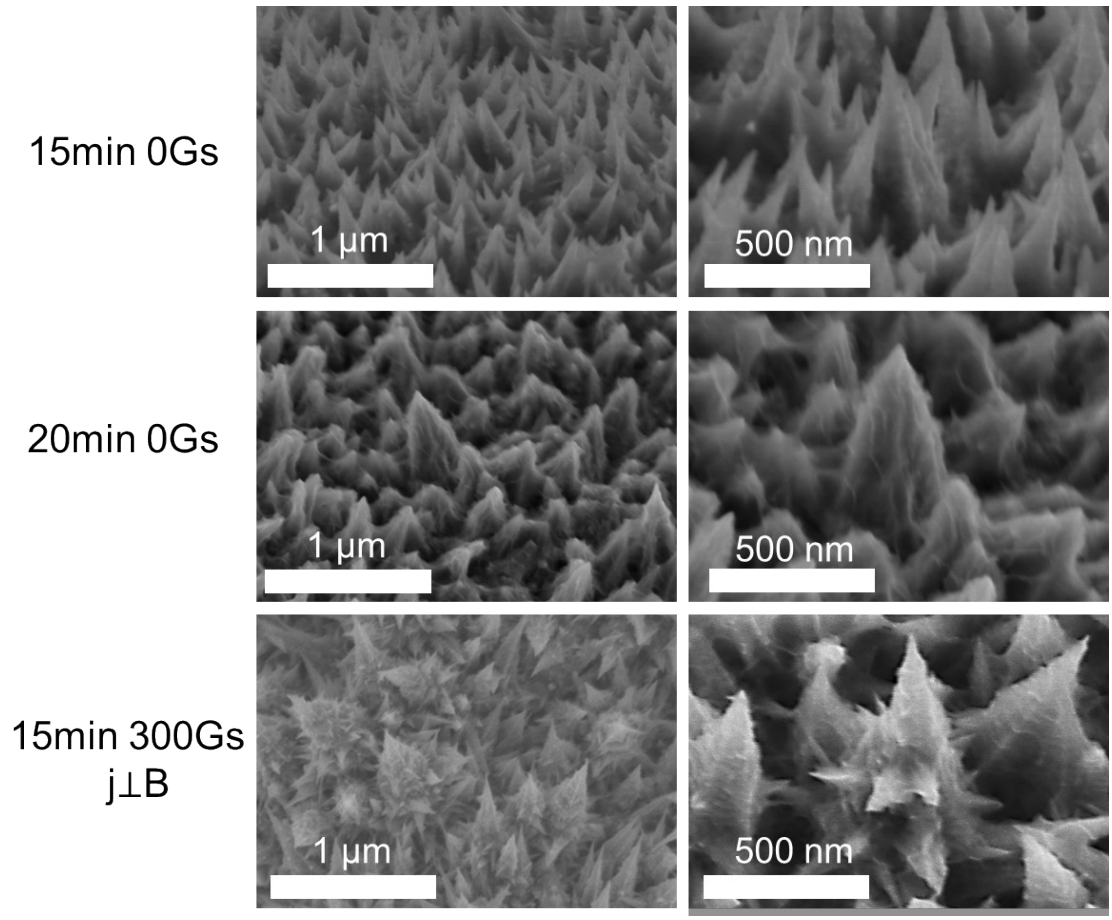

Fig. S1 Nanocone morphology under different electrodeposition conditions. The experimental conditions for the electrodeposition were as follows: pH of 4.0, current density of 20 mA cm^{-2}. The direction of the magnetic field is perpendicular to the direction of the current.

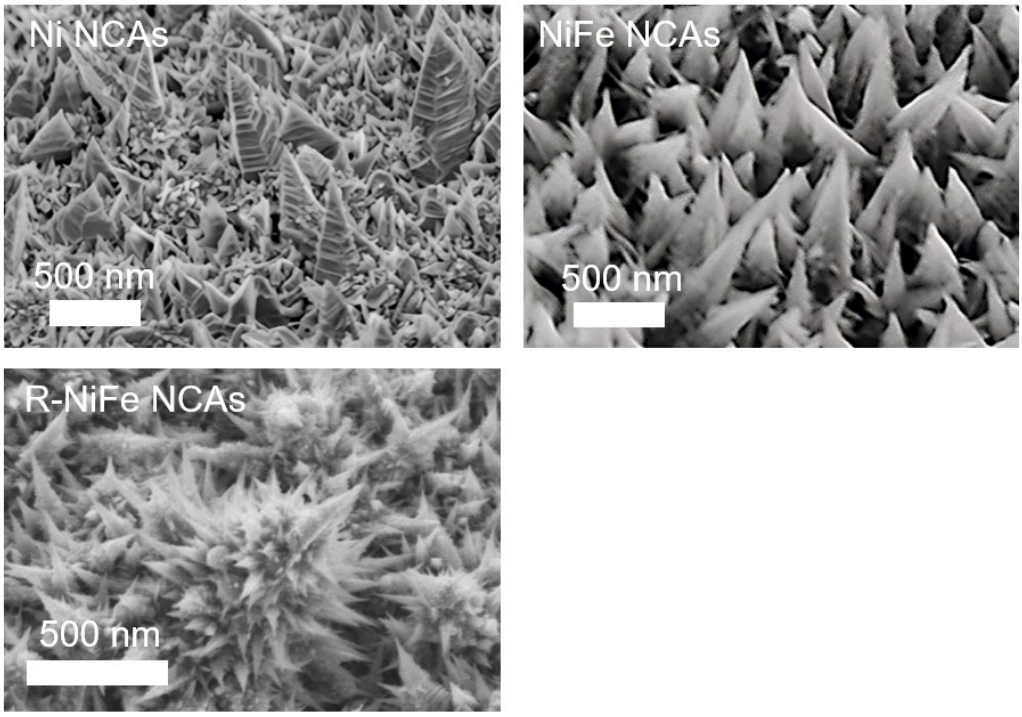

Fig. S2 SEM images of three types of nanocones: Ni NCAs, NiFe NCAs, and R-NiFe NCAs.

500 nm

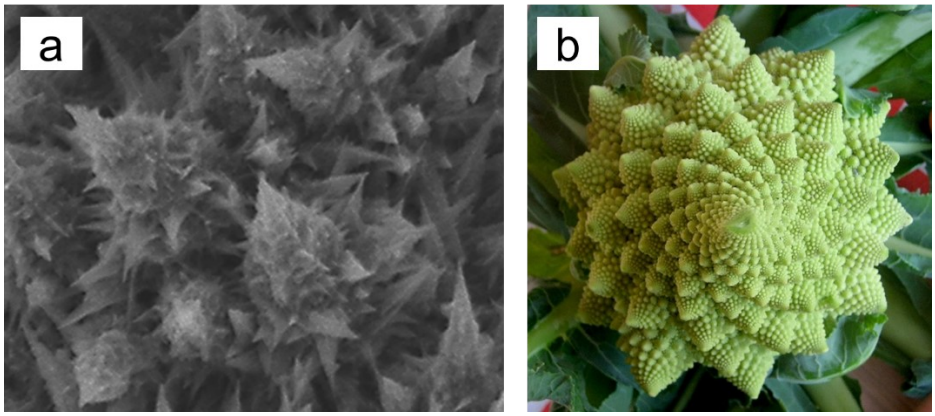

Fig. S3 (a) Romanesco-like Ni-Fe nanocones and (b) biomimetic structures.
(Figure b. Reproduced from Conoce Hidroponía on 27 enero, 2016)

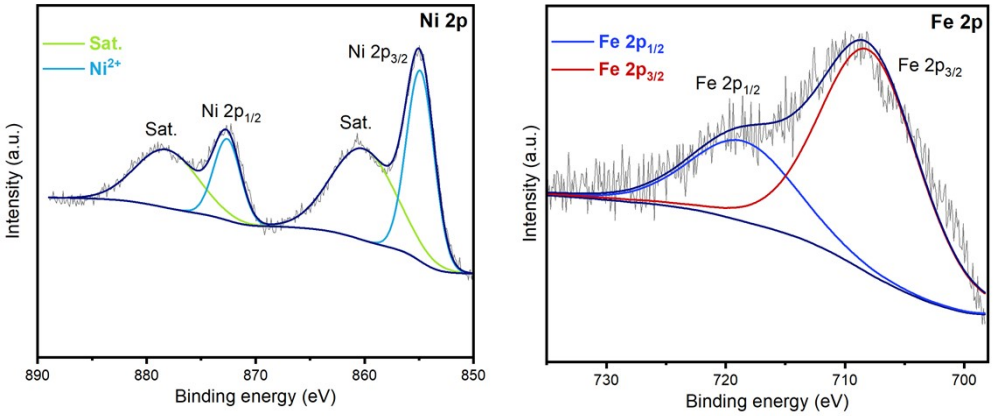

Fig. S4 Surface XPS fitting spectra of R-NiFe NCAs (oxidized layer).

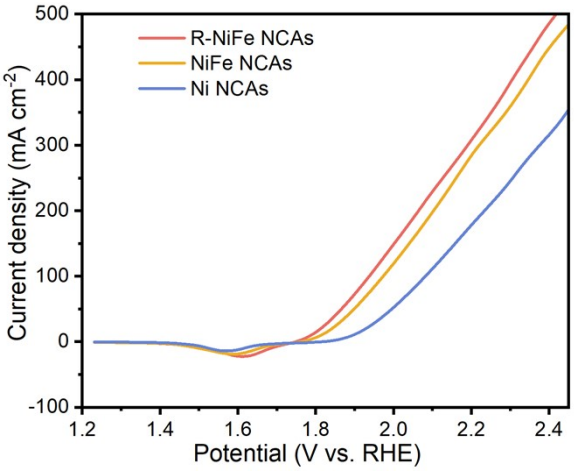

Fig. S5 The polarization curves of R-NiFe NCAs, NiFe NCAs, and Ni NCAs for OER without iR compensation.

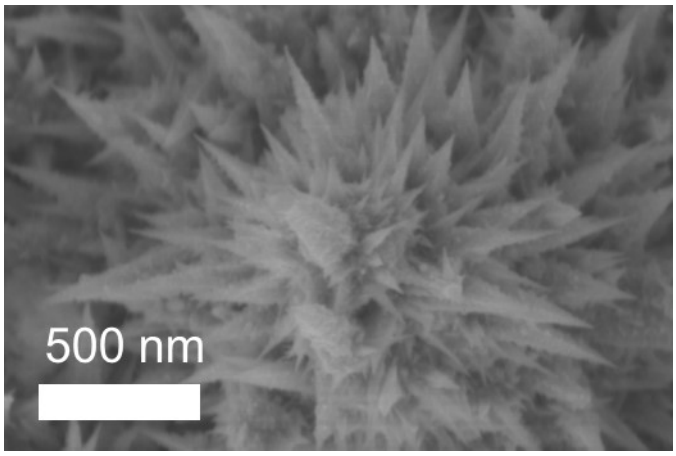

Fig. S6 SEM images of the surface nanocone morphology of R-NiFe NCAs after OER reaction

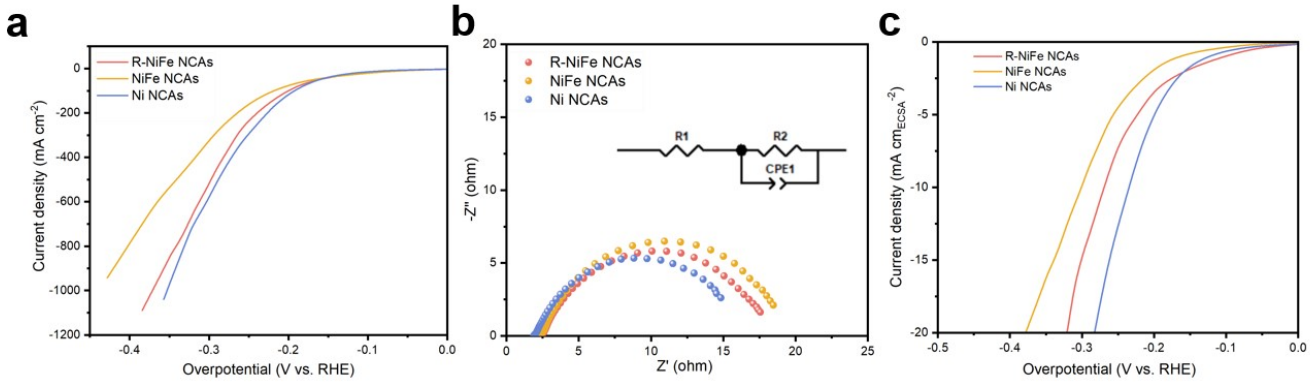

Fig. S7 Comparison of HER electrocatalytic performance of R-NiFe NCAs, NiFe NCAs, and Ni NCAs electrodes in 1 mol L^{-1} KOH solution. (a) Polarization curves based on geometric area, (b) EIS Nyquist plot at 100 mV HER overpotential, (c) Polarization curves based on ECSA.

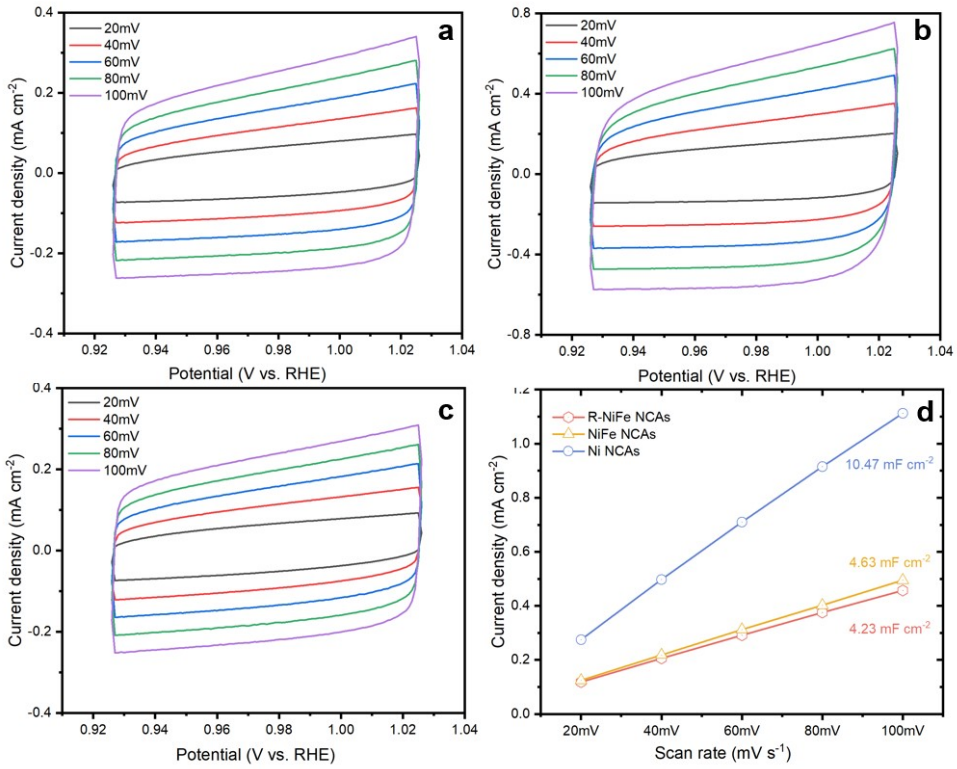

Fig. S8 CV curves at different scan rates (20, 40, 60, 80, 100mV s^{-1}) of (a) NiFe NCAs and (b) Ni NCAs, (c)R-NiFe NCAs. (d) Cdl calculations of NiFe NCAs, Ni NCAs and R-NiFe NCAs.

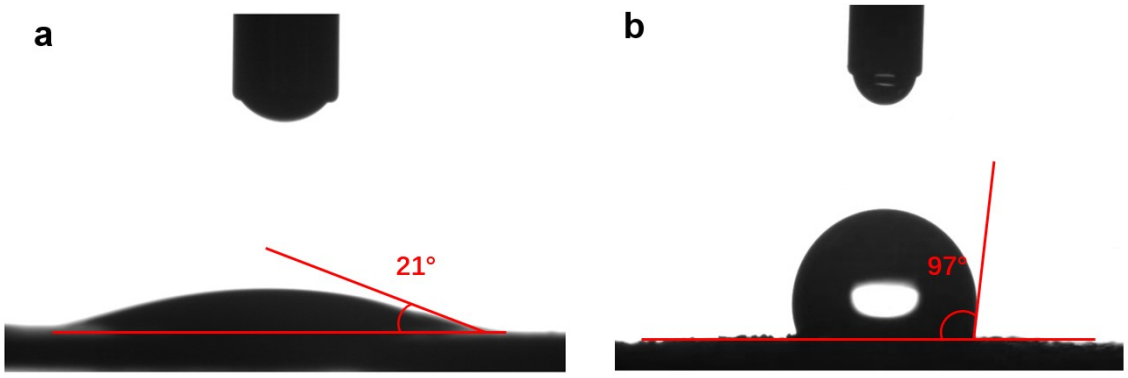

Fig. S9 (a)R-NiFe NCAs and (b) NiFe NCAs contact angle experiments.

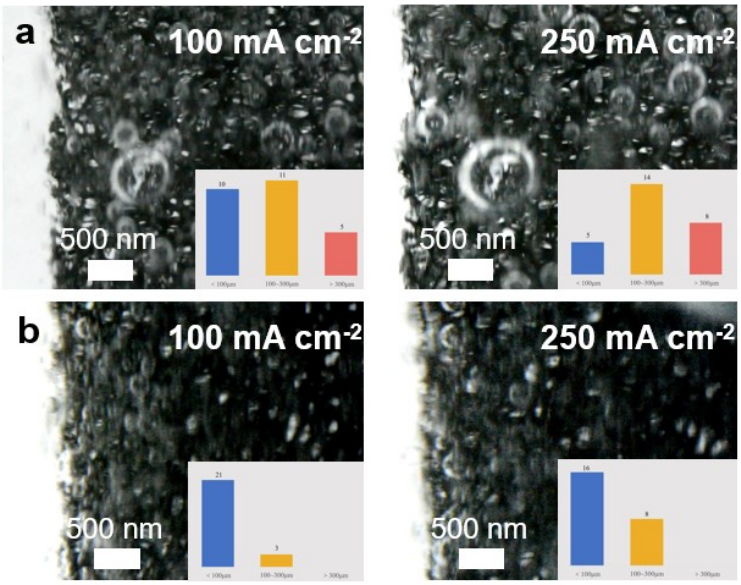

Fig S10. (a) NiFe NCAs and (b) R-NiFe NCAs statistical distribution of oxygen bubble diameters during the OER process at different current densities. The bubble detachment behavior was analyzed using high-speed imaging during chronoamperometry tests at 100 mA cm^{-2} and 250 mA cm^{-2}. Images were captured 30 seconds after the reaction started to ensure consistent conditions.

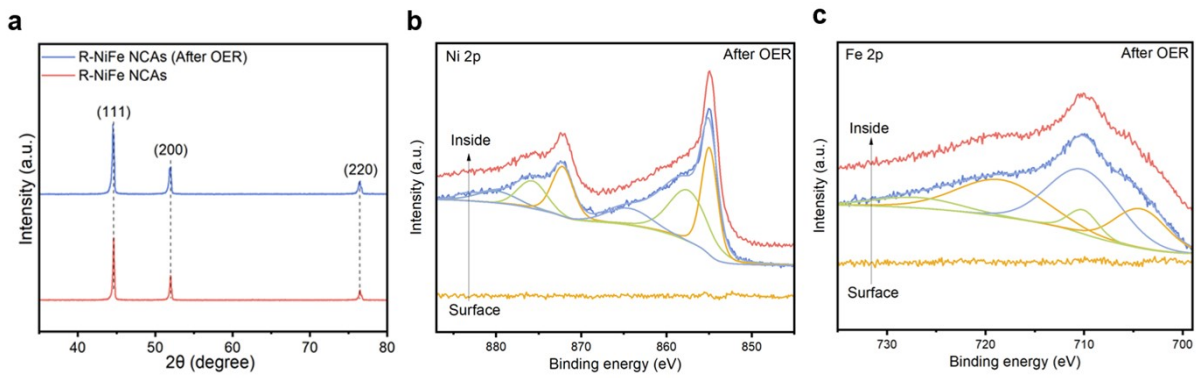

Fig S11. (a) XRD patterns , (b) Ni 2p, (c) Fe 2p XPS depth profiling analysis with sputtering depths of 0, 30, and 50 nm of the surface nano-cone morphology of R-NiFe NCAs after OER process.